



**Interfacial nano-mixing in a miniaturized platform enables  
signal enhancement and in situ detection of cancer  
biomarkers**

Journal:	<i>Nanoscale</i>
Manuscript ID	NR-ART-12-2017-009496.R1
Article Type:	Paper
Date Submitted by the Author:	27-Feb-2018
Complete List of Authors:	<p>Wuethrich, Alain; University of Queensland Australian Institute for Bioengineering and Nanotechnology, Centre for Personalised Nanomedicine Sina, Abu Ali Ibn; The University of Queensland, Australian Institute of Bioengineering &amp; Nanotechnology (AIBN)</p> <p>Ahmed, Mostak; University of Queensland Australian Institute for Bioengineering and Nanotechnology, Centre for Personalised Nanomedicine Lin, Ting-Yun; University of Queensland Australian Institute for Bioengineering and Nanotechnology</p> <p>Carrascosa, Laura; australian institute for bioengineering and Nanotechnology,</p> <p>Trau, Matt; University of Queensland, AIBN</p>



## Interfacial nano-mixing in a miniaturised platform enables signal enhancement and in situ detection of cancer biomarkers

Received 00th January 20xx,  
Accepted 00th January 20xx

DOI: 10.1039/x0xx00000x

www.rsc.org/

Alain Wuethrich<sup>a†</sup>, Abu Ali Ibn Sina<sup>a†</sup>, Mostak Ahmed<sup>a</sup>, Ting-Yun Lin<sup>a</sup>, Laura G. Carrascosa<sup>a</sup>, and Matt Trau<sup>a,b\*</sup>

Interfacial biosensing performs the detection of biomolecules at the bare-metal interface for disease diagnosis by comparing how biological species derived from patient and healthy individuals interact with bare metal surfaces. This technique retrieves clinicopathological information without complex surface functionalisation which is a major limitation of conventional techniques. However, it is still challenging to detect subtle molecular changes by interfacial biosensing, and detection often requires prolonged sensing times due to the slow diffusion process of the biomolecules towards the sensor surface. Herein, we report on a novel strategy for interfacial biosensing which involves in situ electrochemical detections under the action of an electric field-induced nanoscopic flow at nanometre distance to the sensing surface. This nanomixing significantly increases target adsorption, reduces sensing time, and enables the detection of small molecular changes with enhanced sensitivity. Using a multiplex electrochemical microdevice that provides nanomixing and in situ label-free electrochemical detection, we demonstrate multiple cancer biomarkers detection on the same device. We present data for the detection of aberrant phosphorylation in EGFR protein and hypermethylation in the EN1 gene region. Our method significantly shortens the assay period (from 40 mins and 20 mins to 3 minutes for protein and DNA, respectively), increases the sensitivity by up to two orders of magnitude, and improves detection specificity.

<sup>a</sup> Centre for Personalized Nanomedicine, Australian Institute for Bioengineering and Nanotechnology (AIBN), Corner College and Cooper Roads (Bldg 75), The University of Queensland, Brisbane QLD 4072, Australia.

<sup>b</sup> School of Chemistry and Molecular Biosciences, The University of Queensland, Brisbane, QLD 4072, Australia

\*Corresponding author

† Equal contribution.

Electronic Supplementary Information (ESI) is available.

## Introduction

Biomolecules undergo significant changes in their structural and functional properties during disease progression.<sup>1–3</sup> While mass spectrometry and sequencing are very expensive for the analysis of these subtle biomolecular changes, recent advancement in nano-biosensing based on microfluidics, surface plasmon resonance, chemiluminescent, and electrochemistry show great promises in providing inexpensive and sensitive alternatives.<sup>4–8</sup> However, most of these techniques rely on time-consuming sensor surface functionalisation which is susceptible to non-specific adsorption of non-target biomolecules and often provides false positive results.<sup>9</sup> Interfacial biosensing is a recently-developed technique that has been reported to overcome the limitation of surface functionalisation because it investigates the direct interaction of biomolecules (e.g. protein, RNA, DNA) with the bare metal surface (i.e., gold) as a mean to extract biomolecular signatures associated with specific diseases. In this technique, disease-specific biomolecular changes are found to affect the way they interact with the surface (e.g. adsorption) resulting in measurable adsorption difference between healthy and diseased biomolecules towards the metal surface.<sup>10,11</sup>

In recent years, we have used the interfacial biosensing to detect aberrant epigenetic (i.e. DNA methylation) and protein post-translational modifications (i.e. phosphorylation) which are highly associated with the onset of cancer.<sup>12–14</sup> However, a general sensing problem with the interfacial system is that the interaction of large biomolecules with the sensing surface is governed by diffusion which is a slow process and can lead to prolonged sensing times. Ideally, a biosensor that is suitable for small volumes of biological samples and specific to register subtle modification to protein and DNA molecules within a short period with higher sensitivity would have broad implication for disease diagnosis and therapy monitoring. Hence, we hypothesise that an interfacial nanomixing facility at the sensor surface could increase the biomolecular interaction reducing the detection time and increasing sensitivity and specificity.

Electric field-induced fluid mixing has recently attracted wide attention and has been applied in biosensing platform for highly specific and sensitive capture of the target biomolecules.<sup>15</sup> The

advantage of electric field-induced fluid nanomixing is that it can be finely tuned to enhance the biomolecular interaction where the target molecules are captured due to their strong affinity to the capture antibody and the non-specifically adsorbed non-target molecules are simultaneously sheared off within a short period of time. However, in most cases, the target molecules were captured on an antibody-functionalised surface and detected by fluorescence microscopy.<sup>16</sup> Fluorescence-based detection of cancer biomarkers such as posttranslational protein modification and DNA methylation can be performed by direct labelling of the target in the complex biological fluid when the labelling probe is highly specific to the target (e.g., immuno-affinity fluorescence probes). However, these probes can be prone to cross reaction with the sample matrix (non-specific interaction) that results in a high background noise. The target signal might also be compromised due to photo bleaching effects. Thus, an adequate step of sample preparation/purification and careful optimisation of the reaction conditions to obtain a reproducible and stable fluorescence signal are generally applied to mitigate these adverse effects. We therefore thought that the integration of interfacial biosensing in a label-free platform providing electric field-induced fluid nanomixing could potentially overcome these major limitations of current biosensing that involve i) prolonged sensing time, ii) surface functionalisation, and iii) the use of labels.

Herein, we present a miniaturised multiplex biosensing platform that combines the nanoscopic fluid flow generation for accelerating sensing time and enhancing specificity followed by in situ label-free electrochemical detection. Using a 4-plex microdevice, we initially show that the electric field potential can be tuned in such a way that it generates a nanoforce to significantly enhance the interaction of biomolecules towards bare gold surface providing significant adsorption output within a brief period. We then validated our platforms in detecting cancer-specific biomolecular modifications such as protein phosphorylation and DNA methylation. Our data shows that our method can differentiate phosphorylated and non-phosphorylated protein as well as methylated and unmethylated DNA in a more robust manner than the previous reports. In addition, our nanomixing-enhanced biosensor shows an up to 200-fold increases in sensitivity and a 13-fold reduction in detection time for detecting these cancer biomarkers. We believe that this miniaturised system holds great promise as multiplex and portable diagnostic device.

## Experimental

### Reagents

Analytical grade bovine serum albumin (BSA), sodium saline citrate 1x (SSC1x, i.e., 150 mM NaCl and 15 mM sodium citrate at pH 7), glycine, and trisaminomethane HCl (Tris HCl) were purchased from Sigma-Aldrich (USA). Lung cancer cell lines of NCI-H1666 and NCI-H1975 were obtained from ATCC (USA) and the cell culture materials such as growth medium (RPMI 1640), fetal bovine serum and antibiotics were provided by Gibco, Life Technologies (Australia). Pierce Classic Magnetic IP/Co-IP Kit containing protein A/G magnetic beads, lysis buffer, elution buffer, and neutralisation buffer were from Thermo Scientific (Australia). Synthetic DNAs were purchased from IBA GmbH (Germany).

### Biosensor fabrication

We fabricated two types of multiplexed devices for protein and DNA detection. The detailed process of device preparation is shown in Electronic Supplementary Information (ESI) Figure S1. The devices were different in the size of the asymmetric electrode pairs. In the design for enhanced protein biosensing, the inner circular electrode was 1000  $\mu\text{m}$  in diameter, then a gap of 1000  $\mu\text{m}$ , and the outer ring electrode had a width of 120  $\mu\text{m}$ . The electrodes employed for DNA biosensing were smaller with an inner circular diameter of 250  $\mu\text{m}$ , a gap of 1000  $\mu\text{m}$ , and outer ring width of 30  $\mu\text{m}$ . Both devices contained four parallel electrodes for multiplexed analysis. The devices were fabricated by the same 2-step standard photolithographic process. The devices were designed using L-Edit Layout Editor V15 from Tanner Research (USA) and written to a 5-inch soda lime chrome mask (Shenzhen Qingyi Precision Mask Making, Singapore). In the first step, negative photoresist AZnLOF 2020 (Microchemicals GmbH) was spincoated on 4-inch borofloat glass wafers (Bonda Technology Pte Ltd., Singapore) for 30 s at 2000 rpm prior a softbake for 2 min at 110  $^{\circ}\text{C}$  and UV exposure at a constant dose of 340 mJ/cm using an EVG 620 mask aligner (Austria). After a post-exposure bake of 1 min at 110  $^{\circ}\text{C}$ , the wafers were developed for 40 s in AZ726 MIF Developer (Microchemicals GmbH, Germany), washed, dried, and oxygen plasma cleaned using a PlasmaPro 80 (Oxford Instruments, United Kingdom) to remove photoresist residues. Next, 10 nm Ti and 200 nm Au were deposited on the wafers using a Temescal FC-2000 electron beam evaporator (Ferrotec, USA). The gold structures of the nanomixing device were then revealed by overnight lift-off in Remover PG (Microchemicals GmbH). In the second step, the whole nanomixing device except the sensing structures was

insulated with negative photoresist similar to the procedure described above. The device fabrication was completed by final cleaning using oxygen plasma.

### Protein extraction and characterisation

To isolate pure EGFR and phosphorylated EGFR (pEGFR) isoforms from the selected lung cancer cell-lines, H1666<sup>EGFR</sup> and HCC827<sup>pEGFR</sup>, we lysed the cultured cells and subsequently performed magnetic immuno-purification (Pierce Classic Magnetic IP/Co-IP Kit containing protein A/G magnetic beads) using a phospho-independent EGFR antibody (Ref. OPA1-10100, Thermo Fischer Scientific, Australia). First, the cultured cells (25 mg) of each cell type was separately incubated with ice cold lysis buffer (25mM Tris HCl pH 7.4, 150 mM NaCl, 1%NP-40, 1 mM EDTA, 5% glycerol) for 5 min with periodic mixing. In this lysis step, protease and phosphatase inhibitors (Ref. 78442, Thermo Fischer Scientific, Australia) was added to the lysis buffer system. Then centrifugation (AllegraX-22 Series Benchtop Centrifuge, Beckman Coulter) at 13,000×g for 10 min was performed to isolate the total protein supernatant from the remaining cell debris pellet. After that, the concentration of the supernatant was measured by using bicinchoninic acid protein (BCA) assay kit (Ref. 23227, Thermo Fischer Scientific, Australia). Next, 1000 µg of total protein was incubated with the affinity-purified phospho-independent EGFR antibody (2 µg) for 1h at room temperature for preparing antibody-antigen complex. Next, this complex was incubated with the pre-washed protein A/G magnetic beads for another 1 h with continuous mixing. Finally 100 µL of elution buffer (0.1M glycine HCl, pH 2.5) was added to the conjugate of protein-antibody-magnetic beads and incubated with continuous mixing for 10 min to isolate EGFR and pEGFR isoforms. In this step, we used a magnetic stand for separating the antibody-anchored magnetic beads from the eluted protein supernatant. Finally, to neutralize the low pH of the elution buffer, 10 µL of neutralisation buffer (1M Tris HCl, pH 8.5) was added to each 100 µL of eluate and then stored at -20 °C with necessary aliquots. The concentration of any eluted protein was quantified by BCA protein assay based on Microplate Reader (BioTek, Synergy HT). The presence of EGFR and phosphorylated EGFR protein were confirmed by Coomassie Blue staining and western blot analysis (see Supplementary information of reference <sup>14</sup>). The immunoprecipitation procedure required approx. 3 h.

### DNA extraction

Genomic DNAs were extracted from  $10^5$  cells plates of BT 474 cells by using DNeasy blood and tissue kit (QIAGEN Pty. Ltd., Venlo, Netherlands) according to manufacturer's instructions. Briefly, the cells were lysed by using lysis buffer to release the nucleic acids and proteins into the solution. The proteins and RNAs were digested using proteinase and RNase enzymes. Subsequently, the solution was centrifuged to remove the digested protein and RNA. The purified DNA was eluted in the elution buffer. A REPLI-g whole genome amplification kit (QIAGEN Pty. Ltd., Venlo, Netherlands) was used to prepare the whole genomic amplified (WGA) DNA by amplifying 50 ng of the human genomic DNA (Roche, Germany) according to manufacturer's instructions. The purified DNAs were stored at  $-20\text{ }^{\circ}\text{C}$ .

### **Bisulfite treatment**

Bisulfite treatment was performed using a MethylEasyXceed kit (Human Genetic Signatures Pty. Ltd., Australia) according to manufacturer's instructions. Briefly, 4  $\mu\text{g}$  of purified DNA were incubated with 150 mM NaOH solution at  $37\text{ }^{\circ}\text{C}$  for 15 minutes followed by treatment with sodium bisulfite at  $80\text{ }^{\circ}\text{C}$  for 45 minutes. The DNA solution containing sodium bisulfite was then mixed with 800  $\mu\text{L}$  of water, 2  $\mu\text{L}$  of glycogen (20 mg/mL, Fermentas, USA) and 1 mL of isopropanol. The mixture was incubated on ice for 30 minutes followed by centrifugation at 14000 g for 10 minutes. The supernatant was removed and washed with 70% ethanol to precipitate the DNA pellet. The washing step was repeated twice to completely remove residual sodium bisulfite salts from the precipitated DNA pellet. The pellet was then re-suspended in elution buffer and desulphonated at  $95\text{ }^{\circ}\text{C}$  for 20 minutes.

### **Asymmetric PCR and sequencing**

To obtain ss-stranded amplified amplicons containing the target sequence, bisulfite treated samples were amplified in a 20  $\mu\text{L}$  reaction containing 1.5 unit Taq DNA polymerase (AmpliTaq DNA Polymerase, Applied Biosystems, Australia), 0.7X PCR buffer (AmpliTaq 10X PCR buffer) 0.2 mM each dNTP, 0.1% tween, 125 nM of forward primer and 375 nM reverse primer (ESI Table S1). Cycling was carried out in a Bio-Rad thermo cycler (MJ Mini Personal Thermal Cycler) using the following conditions: denaturation at  $94\text{ }^{\circ}\text{C}$  for 10 min followed by 35 cycles of  $94\text{ }^{\circ}\text{C}$  for 30 s,  $58\text{ }^{\circ}\text{C}$  for 45 s and  $72\text{ }^{\circ}\text{C}$  for 30 s. Finally, the methylation status of the target sequences was validated by Sanger sequencing (see Supplementary information of reference <sup>17</sup>).

### Nanomixing and in situ electrochemical detection

For nanomixing, the device was connected to a signal generator Agilent Technologies 33510B (USA), 10  $\mu\text{L}$  of sample was added to the electrodes of the 4-plex device, and an alternating current (ac) electric field was applied. The electrodes were then washed with buffer before adding 10  $\mu\text{L}$  of redox probe for electrochemical read-out with a CHI 650D (CH Instruments, USA). The redox solution for differential pulse voltammetry (DPV) was 2.5 mM  $[\text{Fe}(\text{CN})_6]^{3-}$  /  $[\text{Fe}(\text{CN})_6]^{4-}$  (1:1) and 0.1 M KCl in 10 mM phosphate buffered saline at pH 7.4. DPV measurements were performed with a pulse amplitude of 50 mV, a pulse width of 50 ms, a potential step of 5 mV, and pulse period of 100 ms. Target adsorption on the electrode resulted in a decrease in relative current ( $\%i_r$ ) according to equation (1)

$$\%i_r = \frac{i_{\text{baseline}} - i_{\text{target}}}{i_{\text{baseline}}} \times 100\% \quad (1)$$

where  $i_{\text{baseline}}$  is the peak current of the bare electrode,  $i_{\text{target}}$  is the peak current after target adsorption on the bare gold electrode. The relative current differences  $\Delta i_r$  of unmethylated DNA and mDNA and EGFR and pEGFR were calculated using  $\Delta i_r = \%i_r(\text{DNA}/\text{pEGFR}) - \%i_r(\text{mDNA}/\text{EGFR})$ .

## Results and discussion

### Interference-free nanomixing and in situ electrochemical detection

**Scheme 1** shows the enhanced biosensing workflow with integrated nanomixing. Target DNA and protein were extracted and purified from cells following standard procedures (see Experimental section). A droplet (10  $\mu\text{L}$ ) of the prepared targets was then added to the asymmetric ring electrode of the device sensor followed by the application of an alternating current (ac) electric field for nanomixing. Upon application of an ac electric field, an electrical double layer in nanometre proximity to the sensor surface is formed. The electric field and surface charges induce an electroosmotic force on each electrode.<sup>18,19</sup> This force is stronger on the larger electrode which results in a nanoscopic fluid flow directed from the inner smaller to the outer larger electrode. This nanomixing enhances biomolecule adsorption and interaction with the biosensor.<sup>16,20</sup> Following nanomixing, in situ electrochemical detection by DPV was performed. DPV measures the current obtained from the electron transfer reaction of redox



probe (i.e., ferro/ferricyanide,  $[\text{Fe}(\text{CN})_6]^{4-/3-}$ ). Target adsorption on the sensor surface resulted in a decrease in Faradaic current as a function of the adsorbed target quantity (i.e., the higher target adsorption, the less current).

### SCHEME 1

**Scheme 1.** Methodological approach for the detection of cancer biomarkers in a miniaturized multiplex platform using electric field-induced interfacial nanomixing.

The application of nanomixing could result in sensor damage and thus interfere with the subsequent electrochemical read-out. To investigate the framework for interference-free in situ electrochemical biosensing, we studied different nanomixing conditions using two buffers which are most commonly used for protein and DNA analysis. The buffers were 20 mM Tris HCl/20 mM glycine at pH 7 (i.e., protein buffer) and 1x sodium saline citrate at pH 7 (i.e., DNA buffer). Nanomixing was performed for 3 min at 0.8 to 4 V and 500 Hz. DPV was used to characterise the biosensor before and after nanomixing. Biosensor damage (e.g., due to electrolysis) results in reduced or incapable redox probe reaction at the sensor surface.

### FIGURE 1

**Figure 1.** Study of nanomixing ac voltage for interference-free electrochemical detection. Voltammograms were obtained using (a) protein buffer and nanomixing performed at an ac electric field of 4.0 V (green), 3.0 V (orange), 2.0 V (blue), and 1.5 V (red). In (b), the signals were from DNA buffer and nanomixing was performed at an ac electric field of 3.0 V (orange), 2.0 V (green), 1.0 V (blue), and 0.8 V (red). The sensor baseline is shown in black.

**Figure 1** shows the voltammograms from the studied nanomixing conditions. An unchanged DPV signal before and after nanomixing indicated that an interference-free electrochemical sensing was possible under the applied nanomixing parameters. The DPV signal was unchanged when nanomixing was performed using (a) protein buffer at 500 Hz and 1.5 V and (b) DNA buffer at 500 Hz and 0.8 V. Sensor damage occurred at voltages of  $\geq 1.5$  V. A microscope image of a damaged sensor and the corresponding voltammogram are shown in ESI Figure S2. The selected nanomixing parameters were then repeatedly applied to test if sensor damage occurs due to repeated voltage application (ESI Figure S3). The voltammograms remained unchanged when

nanomixing was performed three times for 3 min as shown by <1% RSD of the DPV peak currents (0.88% RSD for protein buffer and 0.52% DNA buffer).

### Demonstration of enhanced sensing using model targets

BSA and synthetic DNA were selected as the model targets to study the concept of nanomixing and in situ electrochemical detection. To investigate the effect of nanomixing time on target adsorption, dilute solutions of BSA (5  $\mu\text{g}/\text{mL}$ ) or synthetic DNA (10 nM) were incubated on the sensor for 2-15 min, and the adsorption levels were finally quantified electrochemically using DPV in the presence of the ferro/ferricyanide redox system. We have previously used this redox system as a quantitative measure of the gold-adsorption levels of DNA<sup>12,21</sup>, and protein molecules<sup>22</sup>. **Figure 2** shows the effect of nanomixing time for (a) BSA and (b) synthetic DNA. Within 3 min of nanomixing, both target adsorptions reached equilibrium. At equilibrium, the relative current decrease  $\%i_r$  was  $41\% \pm 2\%$  and  $44\% \pm 2\%$  for BSA and synthetic DNA, respectively. For comparison, static incubation was also performed (red line). Static incubation is governed by diffusion of the target to the sensor surface, and this process took >1h to reach equilibrium for both biomolecules. At 60 min, the relative current decrease  $\%i_r$  was  $25\% \pm 2\%$  and  $28\% \pm 2\%$  for BSA and synthetic DNA, respectively. The  $\%i_r$  remained constant even at prolonged incubation times of 2h. Thus nanomixing was efficient in stimulating target-sensor interaction and in enhancing the target adsorption and significantly accelerating the sensing time. To investigate the dynamic range and detection limit of the nanomixing-enhanced electrochemical sensor, concentrations of 0.05-50  $\text{ng}/\mu\text{L}$  BSA and 0.2-500 nM synthetic DNA were run on the sensor (ESI Figure S4). The data suggested that the enhanced biosensor was sufficiently sensitive to detect 0.05  $\text{ng}/\mu\text{L}$  BSA and 0.2 nM synthetic DNA.

### FIGURE 2

**Figure 2** shows the relative current mean values dependence on target adsorption time. A buffered solution of (a) 5  $\mu\text{g}/\text{ml}$  BSA and (b) 10 nM synthetic DNA was adsorbed using nanomixing (blue) or static (red) incubation. The error bars represent the standard deviation of three replicates.

### Demonstration of enhanced biosensor for rapid and sensitive detection of cancer biomarkers

To demonstrate the applicability of our enhanced biosensor in detecting different cancer biomarkers, we first sought to investigate phosphorylation status of EGFR protein which is found to be highly associated with cancer progression and metastasis. Recently, we have developed a

protein-bare gold affinity based method that can detect the phosphorylation status of EGFR by simply adsorbing the protein onto the gold electrode.<sup>14</sup> The method relies on phosphorylation-induced conformational changes in EGFR protein providing more affinity towards the gold surface for phosphorylated EGFR in comparison to the non-phosphorylated isoform. Thus, we hypothesised that the use of nanomixing can significantly increase the biomolecular interaction towards gold surface. Simultaneously, the applied electric field may potentially be tuned in such a way that the high affinity phosphorylated protein can adsorb more strongly towards gold electrode while the low affinity non-phosphorylated protein shears off and thereby provide higher sensitivity and faster detection. To perform this assay, we extracted non-phosphorylated and phosphorylated EGFR derived from H1666 and H1975 lung cancer cell lines respectively. While H1666 cells express non-phosphorylated EGFR in the absence of EGFR cognate ligand, H1975 express a mutated EGFR form that results in constitutive ligand-independent auto-phosphorylation (i.e., H1975 carries T790M and L858R mutations respectively on exons 20 and 21). We then adsorbed both the EGFR and phosphorylated EGFR on the gold electrode to perform the interfacial nanomixing followed by electrochemical detection. As shown in **Figure 3**, the microelectrodes in our 4-plex device significantly increased the sensitivity of detection (10 ng/ $\mu$ L) in comparison to the previously reported macroelectrode system even with the static incubation. However, when we applied the ac electric field-induced nanoforce (at optimised conditions of 1.5 V, 500 Hz, and 3 min) to introduce nanomixing of biomolecules within the system at the same concentration, complete saturation of the sensor was obtained providing a flat DPV signal (ESI Figure S5a). Thus, we reduced the concentration and a very significant signal enhancement was achieved requiring only 2 ng of protein to detect the phosphorylation status of EGFR which is a 200-fold reduction in comparison to the previously reported system. More importantly, the signal difference between EGFR and phosphorylated EGFR is significantly increased using nanomixing as shown by the increase in  $\Delta_{ir}$  from 18% to 31%, indicating that our method is very robust in detecting subtle modifications in the protein. In addition, the assay time is considerably reduced from 40 min to 3 min using the nanomixing-enhanced biosensor. These significant efficiency improvements (in terms of sensitivity, specificity, and assay time) were a direct consequence of nanomixing-enhanced interfacial biosensing.

## FIGURE 3

**Figure 3.** Comparison of nanomixing-enhanced biosensor and static biosensor for cancer biomarker detection. The voltammograms of the protein biomarker were obtained from (a) static adsorption of 10 ng/ $\mu$ L pEGFR (blue) and EGFR (red) and (b) nanomixing-enhanced adsorption (EHD conditions; 1.5 V, 3 min) of 0.2 ng/ $\mu$ L pEGFR (blue) and EGFR (red). The signals of nucleic acid biomarker were after (c) static incubation of 5 ng/ $\mu$ L unmethylated DNA (umDNA, red) and methylated DNA (mDNA, blue) and (d) nanomixing-enhanced adsorption (EHD conditions; 0.8 V, 3 min) of 0.5 ng/ $\mu$ L unmethylated DNA (red) and methylated DNA (blue). The inset bar graphs show the relative current change ( $\%i_r$ ) and relative current difference ( $\Delta i_r$ ). The error bars represent the standard deviation of three replicates.

Next, we investigated the potential of our biosensor in detecting gene specific regional DNA methylation. In recent years, we have developed a simple method for detecting regional DNA methylation based on gold-DNA affinity which does not require a sensor surface functionalisation.<sup>12</sup> The method, referred to as Methylsorb, relies on the different adsorption of bisulfite treated and asymmetrically amplified methylated and unmethylated DNA towards bare gold surface. Bisulfite treatment converts the unmethylated cytosine into uracil leaving the methylated cytosine unchanged. The following asymmetric PCR then generates adenine in the antisense strand of unmethylated DNA while in methylated strands it generates guanine. Since gold-DNA affinity follows the A>C>G>T adsorption trend, unmethylated DNA adsorbs strongly towards the gold surface in comparison to the methylated DNA, and this difference in adsorption based on their methylation status has been detected by optical and electrochemical techniques.<sup>12,13</sup> Since Methylsorb can detect the methylation biomarker by direct adsorption of DNA towards the gold surface; we thought to utilise our enhanced biosensor for the detection of DNA methylation. Similarly, in our previous methods, we used the EN1 region which has been recognised as a potential methylation marker for many cancer types. To generate the methylated EN1 template, we used DNA derived from MCF7 breast cancer cell line while for an unmethylated control, we used the same EN1 region derived from whole genome amplified DNA which has no methylation mark present due to the amplification. As shown in Figure 3c, the static incubation for 20 min at 5 ng/ $\mu$ L concentration provided only 16  $\pm$ 3% difference in adsorption between methylated and unmethylated DNA which is in agreement with our previous reports. However, the electric field-induced nanomixing (at optimised conditions of 0.8 V, 500 Hz, and 3 min) at the same concentration provided a flat DPV signal for both methylated and unmethylated DNA suggesting a complete saturation of the sensor surface (ESI Figure S5b). Thus, we reduced the DNA concentration to only 500 pg/ $\mu$ L and a significant difference in adsorption (29  $\pm$ 3%) between methylated and unmethylated DNA was obtained.

Using nanomixing, the assay efficiency was substantially improved as it is given by the reduction in assay time from 20 min to only 3 min. Although our method still required the extraction and purification of target samples from the biological matrix to avoid any non-specific interaction from non-target molecules, this type of sample preparation is common for most of the biosensing techniques. Thus, regardless of the time required for sample preparation, we believe our method provides significant improvement in the efficiency and in situ detection of target molecules in only 3 minutes with remarkable signal enhancement. These improvements in sensitivity, specificity, and read-out time indicate that our method may have a high potential for clinical application.

## Conclusion

A nanomixing-enhanced multiplexed device for label-free detection of cancer biomarkers was demonstrated. The device integrated interfacial biosensing with an ac field-induced fluid flow in nanometre proximity to the sensing surface followed by in situ electrochemical detection. This novel sensing concept was explored for detection of the phosphorylation status of EGFR protein and gene-specific DNA methylation where we achieved an up to 200-fold improvement in sensitivity and 13-fold decrease in sensing time. Further, the adsorption difference between the targets was significantly increased while only requiring minute volumes (10  $\mu\text{L}$ ) and low sample concentrations (0.2  $\text{ng}/\mu\text{L}$ ). The increase in adsorption difference is important since it can more precisely pinpoint protein and DNA modifications. Although the interfacial nanomixing-enhanced sensor was demonstrated for protein phosphorylation and DNA methylation, it can potentially be applied for analysing RNA methylation and other post-translational modifications such as protein glycosylation, acetylation, and ubiquitination. We think that the combination of rapid nanomixing with multiplexed detection will be crucial in obtaining a comprehensive profile of the cellular response to different environments. For instance, the monitoring of multiple protein targets in response to drug treatment and disease progression could also be explored. Finally, we believe that the stimulation of a nanoscopic fluid flow or nanomixing at the interface of sensor surface in combination with label-free electrochemical detection will offer great potential for fast and sensitive detection of cancer biomarkers and integration into the point-of-care environment.

## Conflicts of interest

There are no conflicts to declare.

### **Acknowledgement**

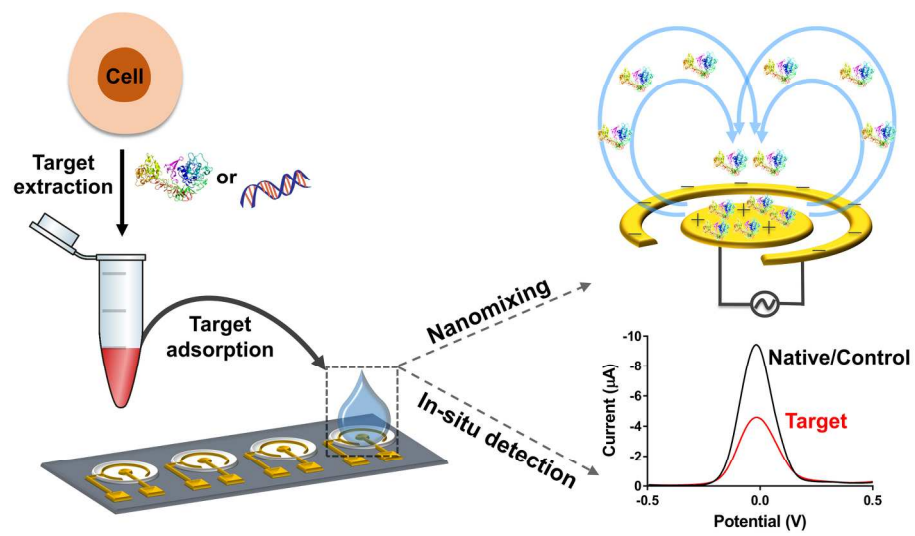
This work was supported by the National Breast Cancer Foundation of Australia (CG-12-07), Swiss National Science Foundation (P2SKP2\_168309), and the UQ Development Fellowship (UQFEL1831057). We also acknowledge the funding from Australian Research Council (DP160102836). These grants have significantly contributed to the environment to stimulate the research described here. Device fabrication was performed at the Australian National Fabrication Facility, Queensland node (ANFF-Q). We also acknowledge Yefei Liang for his contribution in performing electrochemistry experiment.

## References

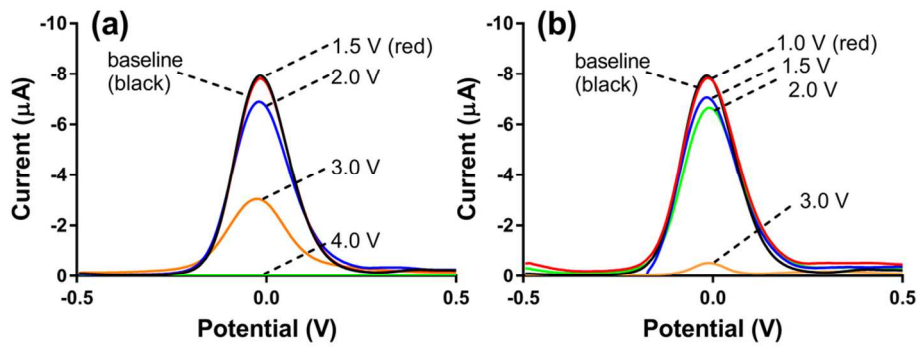
- 1 M. M. Suzuki and A. Bird, *Nat. Rev. Genet.*, 2008, **9**, 465–476.
- 2 D. Schübeler, *Nature*, 2015, **517**, 321–326.
- 3 T. M. Karve and A. K. Cheema, *J. Amino Acids*, 2011, **2011**, 207691.
- 4 Z. Wang and Z. Dai, *Nanoscale*, 2015, **7**, 6420–6431.
- 5 J. Wang and X. Qu, *Nanoscale*, 2013, **5**, 3589–3600.
- 6 P. Jia and J. Yang, *Nanoscale*, 2014, **6**, 8836–8843.
- 7 Y. Chen, J. Sun, Y. Xianyu, B. Yin, Y. Niu, S. Wang, F. Cao, X. Zhang, Y. Wang and X. Jiang, *Nanoscale*, 2016, **8**, 15205–15212.
- 8 J. Wang, W. Lu, C. Tang, Y. Liu, J. Sun, X. Mu, L. Zhang, B. Dai, X. Li, H. Zhuo and X. Jiang, *Anal. Chem.*, 2015, **87**, 11893–11900.
- 9 A. Makaraviciute and A. Ramanaviciene, *Biosens. Bioelectron.*, 2013, **50**, 460–471.
- 10 H. Li and L. Rothberg, *Proc. Natl. Acad. Sci. U. S. A.*, 2004, **101**, 14036–14039.
- 11 H. Li and L. J. Rothberg, *J. Am. Chem. Soc.*, 2004, **126**, 10958–10961.
- 12 A. A. I. Sina, L. G. Carrascosa, R. Palanisamy, S. Rauf, M. J. A. Shiddiky and M. Trau, *Anal. Chem.*, 2014, **86**, 10179–10185.
- 13 A. A. I. Sina, S. Howell, L. G. Carrascosa, S. Rauf, M. J. A. Shiddiky and M. Trau, *Chem. Commun.*, 2014, **50**, 13153–13156.
- 14 M. Ahmed, L. G. Carrascosa, A. A. Ibn Sina, E. M. Zarate, D. Korbie, K. Ru, M. J. A. Shiddiky, P. Mainwaring and M. Trau, *Biosens. Bioelectron.*, 2017, **91**, 8–14.
- 15 R. Vaidyanathan, S. Dey, L. G. Carrascosa, M. J. A. Shiddiky and M. Trau, *Biomicrofluidics*, 2015, **9**, 61501.

- 16 R. Vaidyanathan, S. Rauf, Y. S. Grewal, L. J. Spadafora, M. J. A. Shiddiky, G. A. Cangelosi and M. Trau, *Anal. Chem.*, 2015, **87**, 11673–11681.
- 17 L. G. Carrascosa, A. A. I. Sina, R. Palanisamy, B. Sepulveda, M. Otte, S. Rauf, M. J. A. Shiddiky and M. Trau, *Chem. Commun. (Camb.)*, 2014, **50**, 3585–3588.
- 18 A. B. D. Brown, C. G. Smith and A. R. Rennie, *Phys. Rev. E - Stat. Nonlinear, Soft Matter Phys.*, 2001, **63**, 1–8.
- 19 A. Ramos, A. González, A. Castellanos, N. G. Green and H. Morgan, *Phys. Rev. E. Stat. Nonlin. Soft Matter Phys.*, 2003, **67**, 56302.
- 20 A. Wuethrich, C. B. Howard and M. Trau, *Microchem. J.*, 2018, **137**, 231–237.
- 21 K. M. Koo, A. A. Ibn Sina, L. G. Carrascosa, M. J. A. Shiddiky and M. Trau, *Analyst*, 2014, **139**, 6178–6184.
- 22 S. Yadav, L. G. Carrascosa, A. A. I. Sina, M. J. A. Shiddiky, M. M. Hill and M. Trau, *Analyst*, 2016, **141**, 2356–2361.

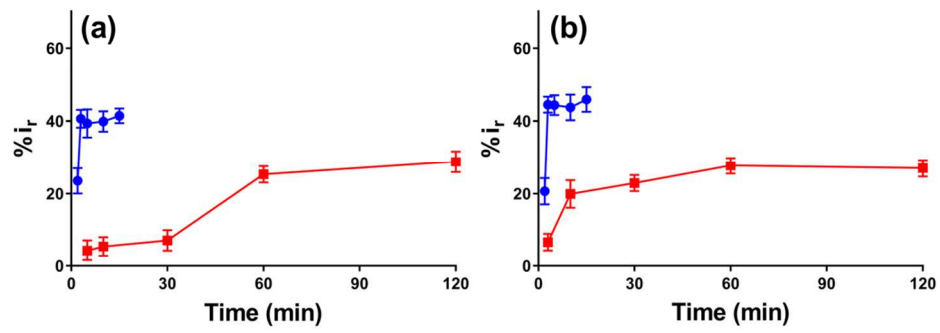




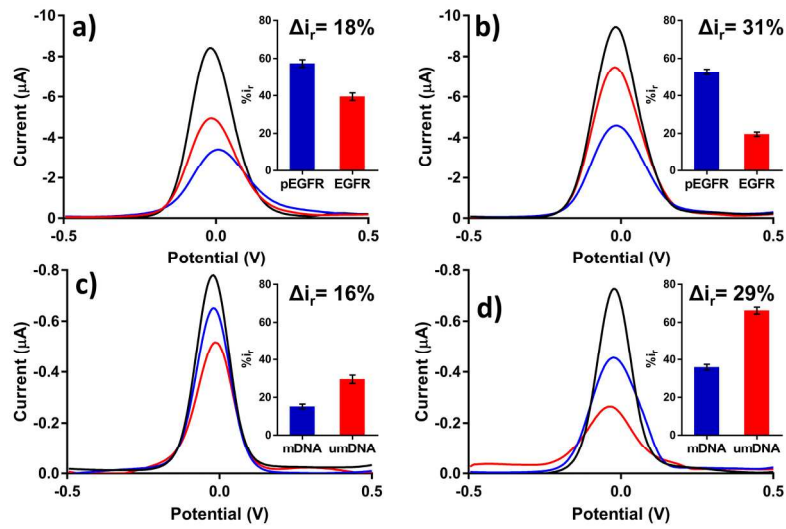
190x107mm (300 x 300 DPI)



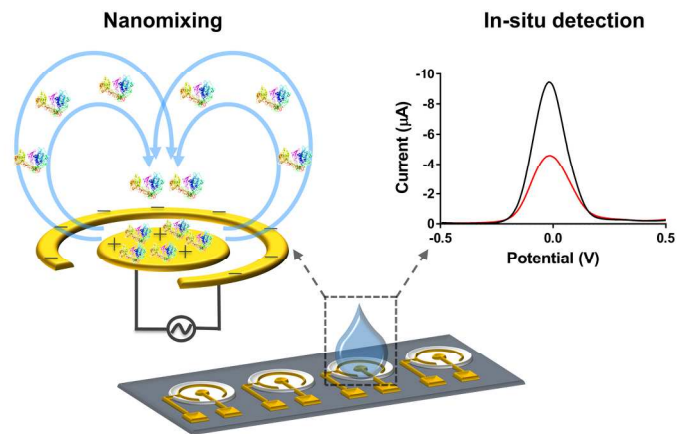
104x41mm (300 x 300 DPI)



106x40mm (300 x 300 DPI)



190x107mm (300 x 300 DPI)



**Interfacial nanomixing enhances the adsorption of cancer biomarkers and provides in-situ electrochemical detection in a multiplexed device.**

190x107mm (300 x 300 DPI)